AJNR

In vivo three-dimensional MR microscopy of mice with chronic relapsing experimental autoimmune encephalomyelitis after treatment with insulin-like growth factor-I.

S Xu, E K Jordan, W Li, Y Yang, S A Chesnick, H D Webster, S Brocke, L Quigley, H F McFarland and J A Frank

AJNR Am J Neuroradiol 1998, 19 (4) 653-658
http://www.ajnr.org/content/19/4/653

AJNR Am J Neuroradiol 19:653–658, April 1998

In Vivo Three-dimensional MR Microscopy of Mice with Chronic Relapsing Experimental Autoimmune Encephalomyelitis after Treatment with Insulin-like Growth Factor-I

Su Xu, E. Kay Jordan, Wen Li, Yihong Yang, Scott A. Chesnick, Henry deF. Webster, Stefan Brocke, Laura Quigley, Henry F. McFarland, and Joseph A. Frank

PURPOSE: **The purpose of this study was to determine the ability of three-dimensional in vivo MR microscopy to depict the treatment effects of insulin-like growth factor-I (IGF-I) in SJL mice with chronic relapsing experimental autoimmune encephalomyelitis (crEAE).**

METHODS: **The experiments were performed at 4.7-T on 10 crEAE mice and on one set of control animals. Five crEAE mice were treated with IGF-I and five were treated with a placebo.**

RESULTS: **In the crEAE mice treated with the placebo, in vivo MR microscopy showed areas of abnormal signal throughout the cerebrum, brain stem, and cerebellum. These findings were not present in either the IGF-I–treated mice or the normal control animals. The diffuse alterations in signal intensity in the placebo-treated crEAE mice were not identified on histologic sections of the same areas.**

CONCLUSION: **Differences between the IGF-I– and placebo-treated groups may reflect changes in stabilization or permeability of cell membranes and/or of the blood-brain barrier, although other alternative contrast mechanisms could be playing a role. In vivo MR microscopy depicted changes resulting from treatment of crEAE with IGF-I.**

Experimental autoimmune encephalomyelitis (EAE) is a model of autoimmune CNS disease characterized clinically by neurologic deficits that occur in a single attack or in a relapsing/remitting pattern. The main histologic features are changes in blood-brain barrier (BBB) permeability, perivascular inflammatory infiltrates, and varying degrees of demyelination accompanied by astrocytic gliosis, relative preservation of axons, and some loss of oligodendrocytes (1, 2). EAE is induced in susceptible animal strains, such as SJL/J mice, by active or passive immunization and is mediated by encephalitogenic T cells (3).

EAE is the most commonly used animal model of multiple sclerosis because of its clinical and pathologic presentation. In the SJL/J mouse model, white matter lesions in different stages of development are present with subacute and chronic lesions. These lesions are often associated with demyelination. Lesions are found most frequently in the spinal cord but are also observed in the brain stem, cerebellum, and cerebrum. Since this model permits assessment of both the clinical and pathologic effects of a given therapy, it has been used frequently to evaluate new treatment strategies for autoimmune inflammatory diseases of the brain (4, 5). When treatment is begun during or after the first attack, effects on clinical deficits and lesion severity can be studied during subsequent exacerbations and remissions (4–6).

In vivo, MR microscopy has been shown to have substantial value in biological and medical studies of small animals (7–11). Its unique, noninvasive, three-dimensional characteristics also permit monitoring of the natural history or treatment effects throughout the course of the disease, thereby minimizing the need to sacrifice valuable animals for histologic studies.

In this study, in vivo MR microscopic images of the brain in normal adult SJL/J mice were compared with images obtained from mice with chronic relapsing (cr)EAE injected with either recombinant human insulin-like growth factor-I (IGF-I), which significantly reduces clinical deficits and lesion severity in crEAE

Received August 5, 1997; accepted after revision October 23.

Cephalon, Inc. provided the insulin-like growth factor-1 used in this study under a material transfer agreement.

From the Laboratory of Diagnostic Radiology Research (S.X., E.K.J., Y.Y., J.A.F.), the Laboratory of Experimental Neuropathology (W.L., H.dF.W.), the Laboratory of Cardiac Energetics (S.A.C.), and the Neuroimmunology Branch (S.B., L.Q., H.F.McF.), National Institutes of Health, Bethesda, MD.

Address reprint requests to Joseph A. Frank, MD, Building 10, Room B1N-256, National Institutes of Health, Bethesda, MD 20892.

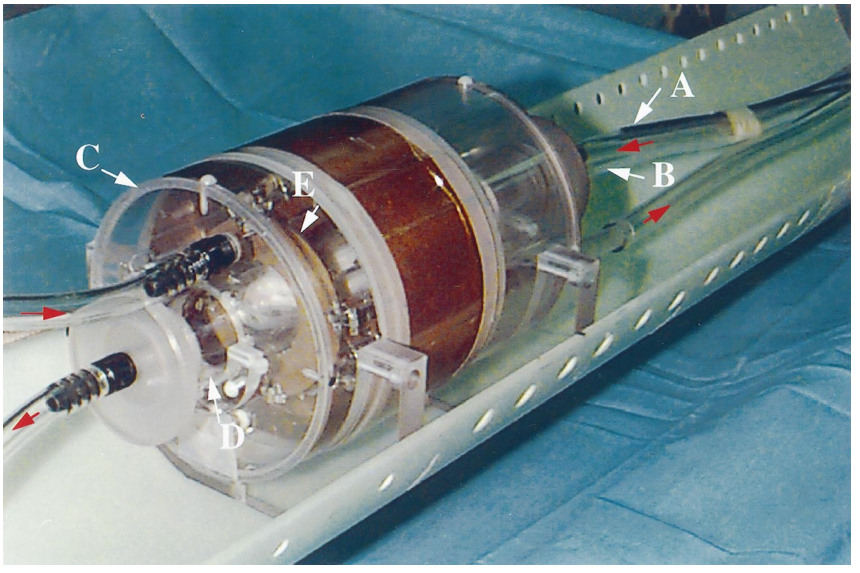

FIG 1. MR microscopy anesthesia chamber and radio frequency coil. (A = optical fibers for temperature measurement, B = pressure sensor, C = outer wall, D = inner wall, E = rf coil; *red arrows* = oxygen/isoflurane mixed air.)

rodent models (12–14), or a placebo. Differences in MR images in IGF-I– and placebo-treated mice were identified and the results compared with the number and area of histologic EAE lesions. The purpose of the study was to determine the ability of 3-D in vivo MR microscopy to depict the treatment effects of IGF-I in SJL mice with crEAE.

Methods

Animal Preparation

The induction of crEAE model preparation in SJL/J mice (Jackson Laboratory, Bar Harbor, Me) by adoptive transfer has been described by Racke and collaborators (15). Briefly, female SJL/J mice, 8 to 12 weeks old, were immunized with guinea pig myelin basic protein (MBP). Draining lymph nodes from MBP-immunized mice were removed and used to prepare a single cell suspension. The lymph node cells were cultured, and 3×10^7 cells were transferred by intravenous injection to each of 10 naive mice, which were then weighed and examined daily for signs of EAE. Clinical disease was scored from 0 to 5 as follows: (0 = normal, 1 = tail weakness, 2 = tail and hind limb weakness, 3 = severe ataxia or moderate paraparesis, 4 = severe quadriparesis, and 5 = moribund). On day 19, after recovering from the first clinically documented EAE attack, the 10 mice were divided into two groups of five each on the basis of closely matched clinical scores. One group received daily subcutaneous injections of 1.2 mg/kg rhIGF-I (a gift of Cephalon, Inc, West Chester, Pa) for 45 days. The other five mice, designated the control group, were given daily subcutaneous injections of a placebo (0.05 mL sodium acetate/acetic acid and sodium chloride buffer, the vehicle for Cephalon's rhIGF-I). The mice were examined by MR microscopy before being studied morphologically after 45 days of treatment with IGF-I or the placebo (day 63 from induction of EAE) then sacrificed. For comparison, MR microscopy also was performed on six age-matched normal adult mice. All procedures met National Institutes of Health guidelines for the care and use of laboratory animals.

MR Microscopy

After inducing anesthesia with an intraperitoneal injection of 0.2 mL of a 1:10 mixture of 65 mg/mL pentobarbital sodium, we placed each mouse prone on a small custom-designed trough. A small balloon filled with deuterium oxide attached to a pressure transducer was placed under the mouse's abdomen, taped in place, and connected to a physiological monitor (Gould, Inc, Cleveland, Ohio) to check respiration. Fiber optic temperature probes (Luxtron, Inc, Mountain View, Calif) were placed along the side of the mouse with the sensor at the level of the head. The head was taped to the trough to maintain positioning. The animal, trough, and sensors were then placed in the MR imaging coil. The coil was sealed, and oxygen and isoflurane (Solvay Animal Health, Inc, Mendota Heights, Minn) anesthetic were run through the chamber and exhausted from the end of the chamber through a vent (Fig 1). The percentage of isoflurane (0.75% to 1.25%) was adjusted to maintain a plane of general anesthesia according to the respiratory rate. The system was prewarmed and its temperature was adjusted to keep body temperature between 24°C and 28°C.

MR microscopic images were obtained on a 4.7-T General Electric CSI Omega NMR spectrometer (Fremont, Calif) with 15-cm (inner diameter) shielded gradients and a custom-designed microimaging bird cage coil. A 3-D fast gradient-recalled echo imaging sequence was used with parameters of 15/5.6/16 (TR/TE/excitations), a 14° flip angle, a $38 \times 19 \times 19$ mm^3 field of view, and a $256 \times 128 \times 128$ imaging matrix. Image resolution was isotropic 150 μm. The parameters were chosen on the basis of the shortest TR/TE with the optimal flip angle to achieve a sufficient signal-to-noise ratio in reasonable experimental time. This resulted in a combination of T1 and proton-density weighting.

After MR imaging, the mice were anesthetized with an intraperitoneal injection of 4% chloral hydrate before perfusing them for 14 minutes with 4% 0.1 mol/L phosphate-buffered paraformaldehyde containing 15% (vol/vol) picric acid. After overnight fixation in the same solution, the brains were removed, cut into 1-mm coronal sections that matched levels illustrated in an atlas of the mouse brain (16), and embedded in paraffin. Sections were cut from the frontal surface of each section and stained with hematoxylin-eosin. To assess demyelination, additional sections were immunostained with a polyclonal antibody to MBP (1:200, Dako, Carpinteria, Calif) and counterstained with methyl green. The MR images were reviewed and compared with matching brain levels shown in paraffin sections. After coding the slides and covering the labels, Bioquant-OS/2 Image Analysis software (Nashville, Tenn) was used to count lesions and measure their areas. Means ± SE of these values were calculated and Student's

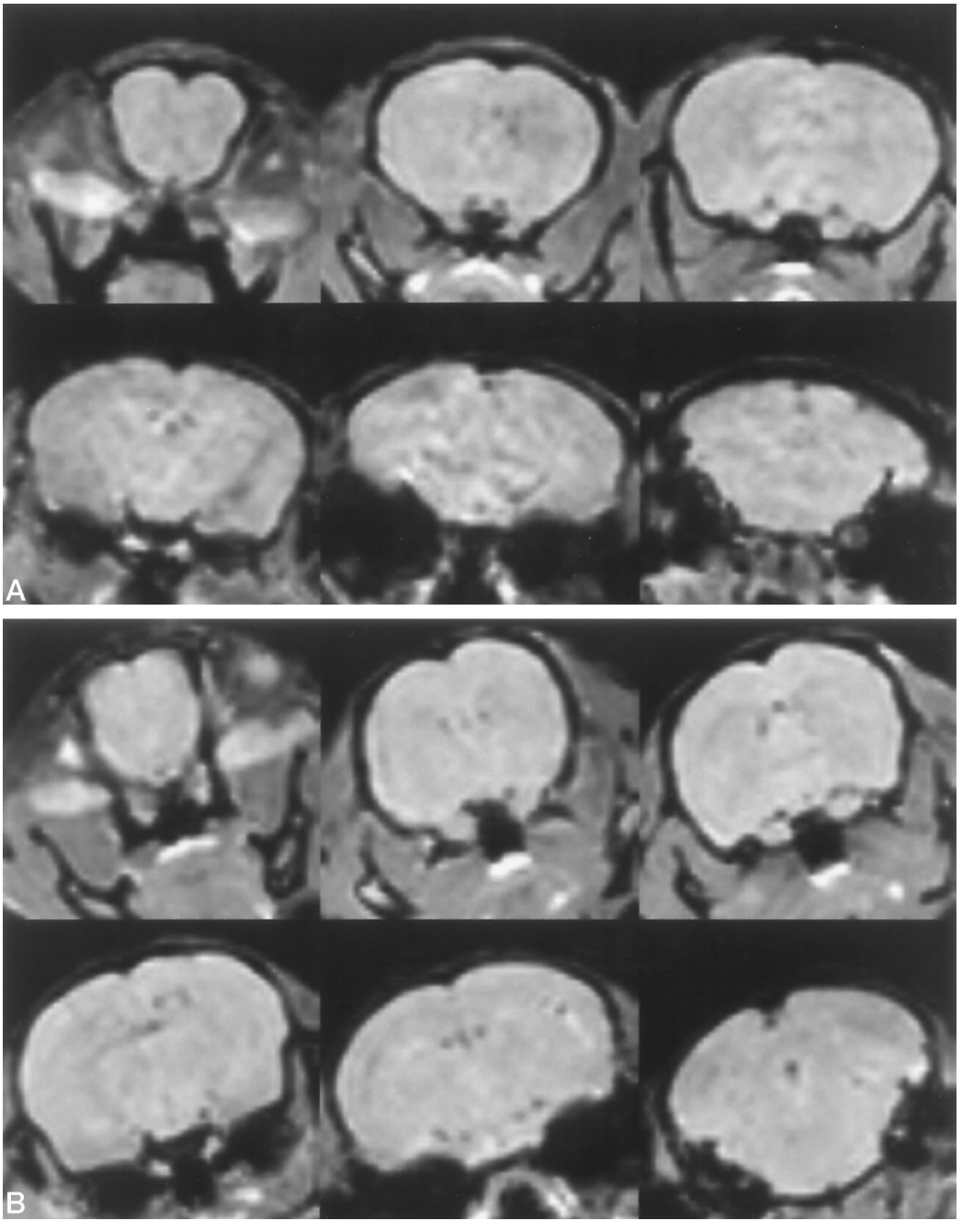

FIG 2. In vivo coronal MR images of the whole crEAE mouse brain on six selected sections with 150-μm spatial resolution isotropic.
A, Placebo-treated mouse. The signal intensity is distributed heterogeneously throughout the brain, from the cerebrum through the cerebellum.
B, IGF-I–treated mouse. The images appear smoother than those of the placebo-treated brain.

t-test was used to determine if lesion values for IGF-I– and placebo-treated mice differed significantly ($P \leq .05$).

Image processing was performed on a Unix workstation using Interactive Data Language software (Research Systems, Inc, Boulder, Colo). For each set of in vivo 3-D MR images, quartile analysis was used for quantification of the SD of the signal intensity divided by the mean signal intensity (SD/mean) over four sections in the frontal parietal region of the brain at the level of the pituitary fossa. In the chosen sections, the signal intensity was measured in defined regions of interest in order to exclude the lateral ventricles. An unpaired Student's *t*-test was used for statistical analysis.

Results

In vivo 3-D MR microscopy of the crEAE mouse brain qualitatively demonstrated areas of inhomogeneous regions of signal intensity in the white and gray matter. These areas were located primarily in the brain stem, cerebellum, and spinal cord, but also in the parietal and frontal lobes. On the MR images, the distribution of signal intensity in the placebo-treated mice was different from that of either the normal or the IGF-I–treated mice. All crEAE mice in this study

had clinical evidence of relapsing-remitting EAE. Figure 2 shows typical examples of in vivo whole-brain MR images in the coronal plane from mice in the placebo- and IGF-I–treated groups. The differences between the two groups are clearly seen in the six selected sections from the different regions of the brain. The signal intensity on the images is more unevenly distributed in most regions of the brain in the placebo-treated crEAE mice than in the IGF-I–treated and normal control mice. Light microscopic examination of paraffin sections showed that the white matter of the cerebrum, cerebellum, and brain stem contained focal lesions consisting of perivascular infiltrates of lymphocytes and mononuclear cells (Fig 3). Focal myelin breakdown was present in some lesion margins (not shown). Compared with the placebo group, the IGF-I–treated group had fewer lesions and they were smaller (Fig 4).

Figure 5 shows MR images from a single section, 150 μm thick, in the frontoparietal region (pituitary fossa level) of a normal mouse and in five mice from the IGF-I–treated group and in five from the placebo-treated group. The clinical scores for the crEAE mice ranged from 0 to 3 when MR imaging was performed.

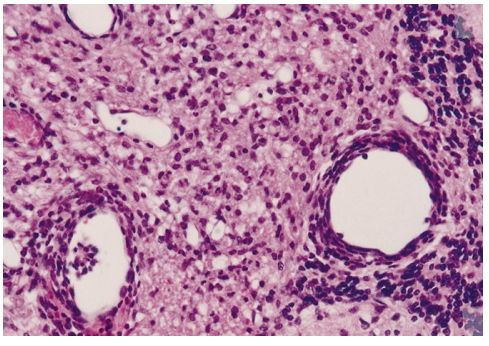

FIG 3. Inflammatory lesion of crEAE at day 63. On the right, there is a large inflammatory lesion with perivascular and parenchymal lymphocytes and mononuclear cells in the white matter and cerebellum. (Hematoxylin-eosin; original magnification ×640.)

As compared with images from the normal mouse and from the IGF-I–treated mice with similar clinical scores, images of the placebo-treated mice had a heterogeneous moth-eaten appearance (Fig 5). Although hematoxylin-eosin and anti-MBP–stained sections of the same areas of the MR images showed differences in the number and size of focal lesions, diffuse changes corresponding to this moth-eaten appearance were not observed. The SD/mean values of signal intensity were calculated for four contiguous sections in the frontoparietal region of the brain at the level of the pituitary fossa (including the section shown in Fig 5) in all animals. Figure 6 shows the quartile analysis of SD/mean values in three groups. The difference in the mean SD/mean values for normal and placebo-treated crEAE mice was highly significant ($P \leq .0001$). In addition, the SD/mean value for IGF-I–treated mice was significantly less than it was in those receiving the placebo ($P \leq .01$) and also did not differ significantly from the mean SD/mean value observed in the normal mice.

Discussion

The EAE adoptive transfer SJL/J mouse model includes pathologic changes characterized by focal lesions in the midbrain, posterior fossa, spinal cord, and, to a lesser extent, the frontoparietal region of the brain (2). In this study, a diffuse component in the pathogenesis of the model was recognized that was distinctly limited to the placebo-treated crEAE mice and that was seen only by MR imaging. Light microscopic examination of paraffin sections did not reveal diffuse abnormalities nor did it indicate possible etiologic mechanisms responsible for these changes. Zhou and colleagues (17) reported similar discrepancies among MR signal changes in the liver of a bromobenzene-induced hepatocellular necrosis model, which preceded histologic changes. They speculated that while image contrast in in vivo MR microscopy is dependent on the proton density and alterations in the relaxation properties of the water within the tis-

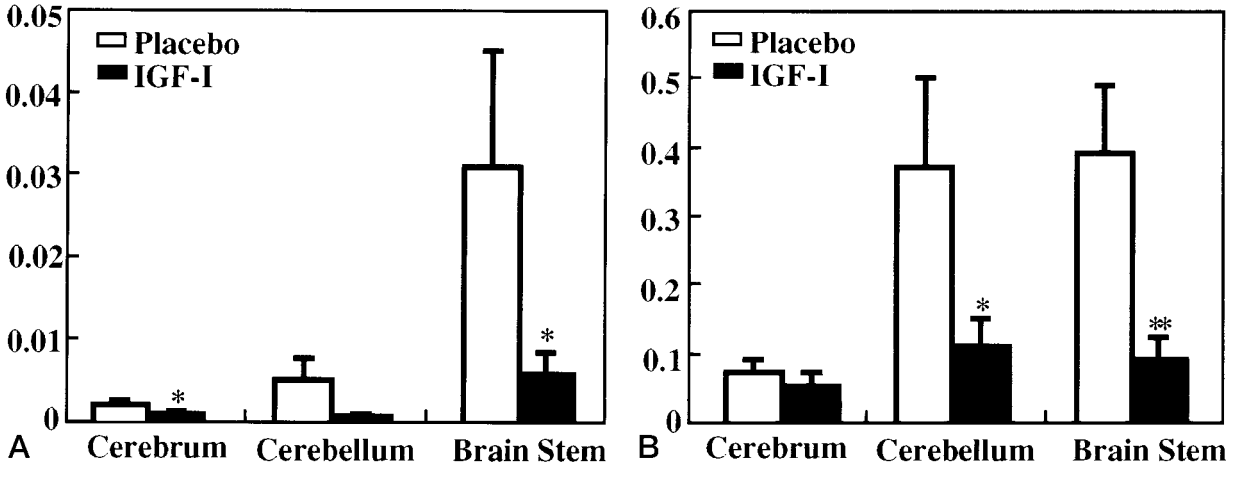

FIG 4. Measurements of inflammatory brain lesions (mm^2/mm^2 section) after 63 days of crEAE. IGF-I treatment for 44 days was started after the first attack (1.2 mg/kg per day, s.c., days 19 to 63). Treatment significantly reduced the area (*A*) and number (*B*) of inflammatory lesions in the cerebrum, cerebellum, and brain stem (*asterisk* = $P \leq .05$).

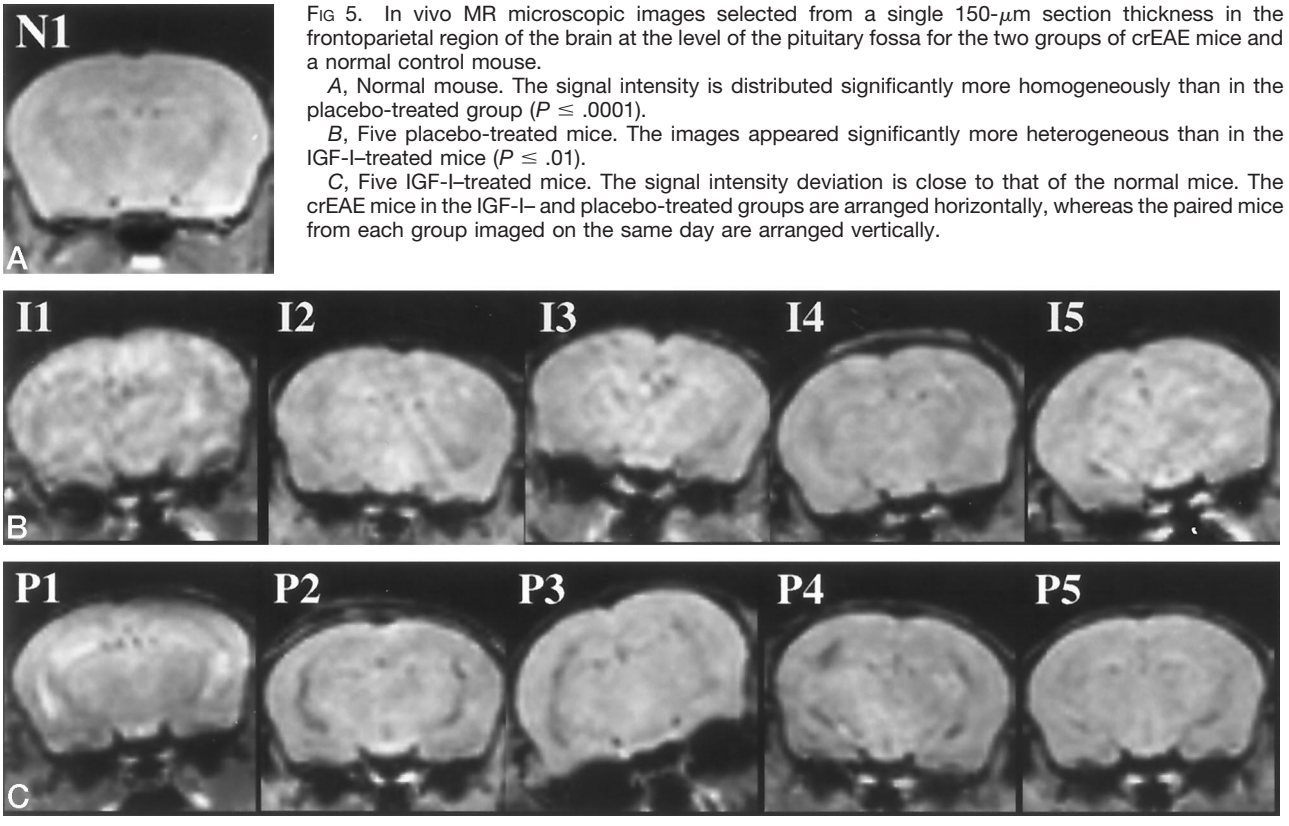

FIG 5. In vivo MR microscopic images selected from a single 150-μm section thickness in the frontoparietal region of the brain at the level of the pituitary fossa for the two groups of crEAE mice and a normal control mouse.

A, Normal mouse. The signal intensity is distributed significantly more homogeneously than in the placebo-treated group ($P \leq .0001$).

B, Five placebo-treated mice. The images appeared significantly more heterogeneous than in the IGF-I–treated mice ($P \leq .01$).

C, Five IGF-I–treated mice. The signal intensity deviation is close to that of the normal mice. The crEAE mice in the IGF-I– and placebo-treated groups are arranged horizontally, whereas the paired mice from each group imaged on the same day are arranged vertically.

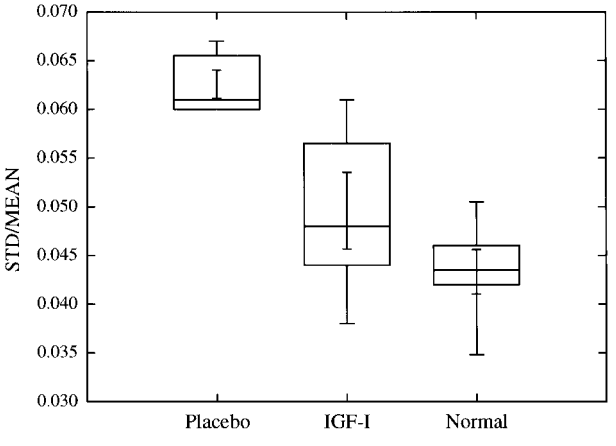

FIG 6. Box plot shows the SD of the signal intensity divided by the mean signal intensity (SD/mean) in the normal, placebo-treated, and IGF-I–treated groups. The box encompasses the 25th through 75th percentiles. *Wide-capped bars* indicate the 10th and 90th percentile points; the *line* marks the value of the 50th percentile. *Narrow-capped bars* represent the standard errors. There is a statistically significant difference between the placebo- and IGF-I–treated groups and between the placebo-treated and normal groups.

sues, pathologic changes in the physiological water environment may be reflected by MR microscopy. These changes, however, would not be apparent by ex vivo histologic examination, because routine histologic staining procedures involve the dehydration of fixed tissues and the binding of stains to macromolecules in cells or tissues. While routine histologic and immunohistologic staining techniques are extremely valuable in identifying inflammation, myelin breakdown, and altered cellular morphology, they are not sensitive to changes in the water and the water-membrane environment within the histologic section (17).

MR detection of signal changes in placebo-treated mice with crEAE that were absent in those treated with IGF-I may reflect the ability of IGF-I to stabilize membrane permeability and prevent changes in the brain's water environment. Known actions of IGF-I in EAE include stabilization of BBB integrity, reduction of inflammatory lesion severity, and promotion of myelin regeneration (12–14). These IGF-I effects may have contributed to the differences noted in the diffuse signal intensity changes between placebo- and IGF-I–treated mice with crEAE. An important finding in this study is that IGF-I–treated and normal control mice had very similar signal intensity patterns and SD/mean values, suggesting that water relaxation times or diffusion coefficients were similar. These results suggest that the IGF-I–treated animals had a reduced lesion severity and reduced BBB permeability as compared with the placebo-treated animals. Li et al (14) showed that these types of histologic findings (ie, reduced lesion severity and BBB permeability) are present in crEAE mice treated with IGF-I, which may have important implications for future trials in patients with multiple sclerosis. Morrissey and colleagues (18) reported the partial inhibition of adoptive EAE transfer in rats by using monoclonal antibodies to intercellular adhesion molecule-1 (ICAM-1). In their study, the untreated EAE rats had

a significant increase in T1 relaxation time in the areas of the medulla and midbrain compared with rats treated with ICAM-1, whereas the treated and normal control animals had no differences 7 days after treatment. In a second study (19), these authors found that changes in the T1-weighted images of their placebo-treated EAE rats paralleled the histologic presence of albumin in brain sections. Other studies in myelin-deficient mutant mice ex vivo have also demonstrated changes in T1 and T2 values, which were consistently longer in the mutant mice than in age-matched control animals (20).

Although the imaging techniques and EAE models in this and the aforementioned study are different, one could postulate that there are possible differences in the relaxation times in brain tissues between IGF-I– and placebo-treated crEAE animal models. Distribution of relaxation times throughout the brain could account for the differences in the appearance of the MR images and the SD/mean value of the signal intensity for the placebo-treated crEAE mice as compared with the normal control or IGF-I–treated animals (Figs 2 and 5). However, further work involving in vivo T1 determination in a separate group of animals would be required to test this theory. The changes observed on MR images may also in large part be attributed to an altered physiological water balance because of EAE pathogenesis producing BBB disruption, inflammatory responses, and structural changes in myelin composition. These changes would therefore be more prominent in placebo-treated crEAE mice, as evidenced by the degree of inflammation and demyelination on histopathologic studies (14).

Conclusion

Although the different appearance in the MR microscopic images of placebo- versus IGF-I–treated mice with crEAE is not fully understood, our results indicate an abnormal characterization of gray and white matter at a macroscopic bulk water level. The MR relaxation times and water diffusion coefficient in this animal model will be investigated to gain a better understanding of the image contrast mechanism found in this study.

Acknowledgments

This work was performed in the In Vivo NMR Research Center at the National Institutes of Health. We thank Alan Olson and Daryl DesPres for their technical support with the experimental hardware.

References

1. Lublin FD. **Experimental models of autoimmune demyelination, In: Cook SD, ed.** *Handbook of Multiple sclerosis.* 2nd ed. New York: Dekker; 1996:122
2. Raine CS, Mokhtarian F, McFarlin DE. **Adoptively transferred chronic relapsing experimental autoimmune encephalomyelitis in the mouse: neuropathologic analysis.** *Lab Invest* 1984;51:534–546
3. Martin R, McFarland HF. **Immunological aspects of experimental allergic encephalomyelitis and multiple sclerosis.** *Crit Rev Clin Lab Sci* 1992;32:121–182
4. Racke MK, Sriram S, Carlino JC, Cannella B, Raine CS, McFarlin DE. **Long-term treatment of chronic relapsing experimental allergic encephalomyelitis by transforming growth factor-β2.** *J Neuroimmunol* 1993;46:175–184
5. Racke MK, Burnett D, Pak S-H, et al. **Retinoid treatment of experimental allergic encephalomyelitis: IL-4 production correlates with improved disease course.** *J Immunol* 1995;154:450–458
6. Stone LA, Frank JA, Albert PS, at al. **The effect of beta interferon on blood brain barrier disruptions demonstrated by contrast enhanced MRI in relapsing remitting multiple sclerosis.** *Ann Neurol* 1995;37:611–619
7. Johnson GA, Benveniste H, Black RD, Hedlund LW, Maronpot RR, Smith BR. **Histology by magnetic resonance microscopy.** *Magn Reson Q* 1993;9:1–30
8. Zhou X, Magin RL, Alameda JC Jr, Reynolds HA, Lauterbur PC. **Three-dimensional NMR microscopy of rat spleen and liver.** *Magn Reson Med* 1993;30:92–97
9. Kapadia RD, High WB, Soulleveld HA, Bertolini D, Sarkar SK. **Magnetic resonance microscopy in rat skeletal research.** *Magn Reson Med* 1993;30:247–250
10. Smith BR, Johnson GA, Groman EV, Linney E. **Magnetic resonance microscopy of mouse embryos.** *Proc Natl Acad Sci U S A* 1994;91:3530–3533
11. Mellin AF, Cofer GP, Smith BR, Suddarth SA, Hedlund LW, Johnson GA. **Three dimensional magnetic resonance microangiography of rat neurovasculature.** *Magn Reson Med* 1994;32:199–205
12. Liu X, Yao D-L, Webster HdeF. **Insulin-like growth factor I treatment reduces clinical deficits and lesion severity in acute demyelinating experimental autoimmune encephalomyelitis.** *Mult Scler* 1995;1:2–9
13. Yao D-L, Liu X, Hudson LD, Webster HdeF. **Insulin-like growth factor I given subcutaneously reduces clinical deficits, decreases lesion severity and upregulates synthesis of myelin proteins in experimental autoimmune encephalomyelitis.** *Life Sci* 1996; 58:1301–1306
14. Li W, Quigley L, Yao D-L, et al. **Early insulin-like growth factor-I treatment reduces clinical deficits and lesion severity in relapses of chronic experimental autoimmune encephalomyelitis.** *Ann Neurol* 1996;40:514
15. Racke MK, Dhib-Jalbut S, Cannella B, Albert PS, Raine CS, McFarlin DE. **Prevention and treatment of chronic relapsing experimental allergic encephalomyelitis by transforming growth factor-b_1.** *J Immunol* 1991;146:3012–3017
16. Sidman RL, Angevine JB Jr, Pierce ET. *Atlas of the Mouse Brain and Spinal Cord.* Cambridge: Harvard University Press; 1971
17. Zhou X, Maronpot RR, Hedlund LW, Cofer GP, Johnson GA. **Detection of bromobenzene-induced hepatocellular necrosis using magnetic resonance microscopy.** *Magn Reson Med* 1995;34:853–857
18. Morrissey SP, Deichmann R, Syha J, et al. **Partial inhibition of AT-EAE by an antibody to ICAM-1 clinico-histological and MRI studies.** *J Neuroimmunol* 1996;69:85–93
19. Morrissey SP, Stodal H, Zettl U, et al. **In vivo MRI and its histological correlates in acute adoptive transfer experimental allergic encephalomyelitis.** *Brain* 1996;119:239–248
20. Jolesz FA, Kirschner DA, Jakab P, Lorenzo AV. **Proton magnetic resonance in myelin deficient brains of mutant mice.** *J Neurosci* 1989;91:85–96